

Superheating of Bi(0001)

E. A. Murphy

*Laboratory for Laser Energetics, University of Rochester, 250 East River Road, Rochester, New York 14623-1299
and Department of Physics and Astronomy, University of Rochester, Rochester, New York 14627*

H. E. Elsayed-Ali

*Laboratory for Laser Energetics, University of Rochester, 250 East River Road, Rochester, New York 14623-1299
and Department of Electrical and Computer Engineering, Old Dominion University, Norfolk, Virginia 23529*

J. W. Herman

*Laboratory for Laser Energetics, University of Rochester, 250 East River Road, Rochester, New York 14623-1299
and Department of Physics and Astronomy, University of Rochester, Rochester, New York 14627*

(Received 17 May 1993)

Superheating of Bi(0001) by about 90 K above the bulk melting temperature is observed using time-resolved reflection high-energy electron diffraction with ~ 200 -ps time resolution. Larger temperature excursions above the bulk melting temperature result in melting accompanied by irreversible laser damage to the surface. The rhombohedral structure of Bi leads to very different behavior of material parameters upon melting as compared with fcc metals. Therefore, our observation of the superheating of Bi(0001), together with the previously observed superheating of Pb(111), suggests the generality of the superheating phenomenon.

Undercooling of liquids is often observed; however, superheating of metals has only been observed under special conditions. The difficulty in superheating metals is attributed to the presence of nucleation sites for melting, such as crystal defects and free surfaces. For many metal surfaces, the formation of a surface-disordered layer below the bulk melting temperature provides a barrier to superheating. The role of the surface in the melting process can be suppressed by working with small crystallites with predominantly close-packed surfaces that are less susceptible to disorder. Small crystallites of exposed Pb(111) facets^{1,2} (0.01–0.5 μm in diameter) and Bi(0001) facets^{3,4} (0.07–0.15 μm in diameter) have been superheated by 2–3 and 7–10 K, respectively. Superheating has also been observed in cases where the nucleation of the melt at the free surface is suppressed. Superheating of Ag by at least 7.5 K has been observed for 120- to 160- μm -diam spheres of Ag coated uniformly with an 11- μm layer of Au.⁵ In other experiments, superheating by ~ 2 K was achieved by preferentially cooling the surface of Sn and Cu rods while internally heating the bulk.^{6,7} Superheating by tens to hundreds of degrees has been reported for metals and noble gases implanted in substrates with higher melting temperatures.^{8,9} More recently, superheating of the Pb(111) surface by ~ 120 K above the bulk melting temperature of 601 K has been observed using ~ 200 -ps time-resolved reflection high-energy electron diffraction (RHEED). In this case, melting of the free surface is bypassed by rapid heating and cooling of the surface with a pulsed laser.¹⁰ A similar time-resolved study on Pb(110) showed that surface melting could not be bypassed with laser heating at the heating and cooling rates used in the experiment.¹¹

Here we report on a superheating study of Bi(0001) us-

ing time-resolved RHEED with ~ 200 -ps time resolution. Bi was chosen because of its relatively low melting temperature ($T_m = 544$ K) and low vapor pressure ($\sim 2 \times 10^{-10}$ Torr) at the melting point, and the fact that previous slow-heating experiments have demonstrated superheating of Bi crystallites. Some of these Bi crystallites melted after a time delay of about 30 min when held at T_m and after about 10 min when held at $T_m + 5$ K.^{3,4} Using time-resolved RHEED with ~ 200 -ps resolution we are able to achieve heating rates of $\sim 10^{11}$ K/s, approximately 13 orders of magnitude larger than that used in the Bi crystallite experiments. In addition, because of the open pseudocubic crystal structure of Bi, liquid Bi is more dense than the solid, and it has been suggested that such unusual structural differences between a crystal and its melt may provide a barrier for rapid melting.¹²

We have observed superheating of Bi(0001) by about 90 K. Larger temperature excursions above T_m result in melting and irreversible laser damage to the surface. Scanning electron microscopy (SEM) images show the presence of a laser-induced periodic surface structure in the damaged region of the sample, the spacing of which is approximately the heating laser wavelength ($\lambda = 1.06$ μm). Significant and irreversible reduction in surface quality is observed, both as a decrease in RHEED streak intensity and as a visible dulling of the surface. We measure a decrease in the reflectivity of the surface at the laser wavelength as a result of the laser damage.

In our experiment a Nd:YAG laser pulse (where YAG denotes yttrium aluminum garnet) is split into two beams. The fundamental wavelength ($\lambda = 1.06$ μm) is amplified and used for heating of the surface at near-normal incidence while a small portion of the beam is frequency quadrupled ($\lambda = 0.266$ μm) and is incident on the

cathode of a photoactivated electron gun, generating a pulsed electron beam. The repetition rate of the laser is about 15 Hz and its pulse width is ~ 200 -ps full width at half maximum (FWHM). The electron energy is 15.0 keV and the width of the electron pulse is comparable to that of the fundamental laser pulse. The electron pulses interact with the sample at glancing incidence to generate the RHEED pattern. By optically delaying the heating laser pulse relative to the electron pulse the time evolution of surface heating can be studied. The diameter of the heating laser beam is ~ 1 cm, measured at FWHM, which is large enough to illuminate the entire sample. The RHEED pattern is lens coupled from a microchannel plate/phosphor-screen assembly to a linear-array detector. A RHEED streak is then monitored by a line scan perpendicular to the streak and through its peak intensity. A mechanical shutter is placed in the path of the heating laser beam allowing the averaging of line scans of heated and unheated streaks in separate memories. Shot-to-shot laser fluctuations as well as long-term fluctuations in the intensity of the electron beam are compensated for by normalizing the streak intensity associated with the heated surface to that associated with the unheated surface $I/I(T_{\text{bias}})$ and averaging over ~ 800 laser shots for each scan. Long-term heating laser fluctuations are controlled to within $\pm 10\%$. The spatial nonuniformity of the beam across the sample is determined to be $\pm 15\%$ using a two-dimensional array detector. Our time-resolved temperature measurements are a result of the convolution of the temporal profile of the electron pulse with that of the surface temperature. The convolution effects are more significant for times where the rate of change of temperature with time is largest. This effect is not accounted for in our analysis, and, as a result, the peak surface temperature induced by the laser is actually somewhat larger than what is reported here. The experimental technique is further described in Ref. 13.

Two Bi(0001) samples were used for these experiments. The single crystals were grown from bismuth of 99.999% purity. The samples were cut to within $\pm 1^\circ$ of the (0001) surface. The surface was then mechanically lapped to a $1\text{-}\mu\text{m}$ finish and chemically etched in 20% HNO_3 followed by 10% HCl . The angle of incidence was approximately $1^\circ\text{--}2^\circ$, corresponding to a probe depth of $1\text{--}3$ Å. In both cases, the electron beam is incident along the $[10\bar{1}0]$ direction. Base pressure in the ultrahigh vacuum system is in the low 10^{-10} -Torr range. Surface cleanliness is checked with Auger electron spectroscopy. Before each experiment, the sample is cleaned with argon-ion bombardment and annealed to 523 K.

In order to relate a given decrease in RHEED streak intensity to a temperature rise ΔT , we obtain an intensity versus temperature calibration. The sample is mounted on a resistively heated Mo stage, and the temperature is monitored by a thermocouple mounted on the surface. The thermocouple was calibrated to the freezing and boiling temperatures of water and to the melting temperature of Pb under vacuum measured in a previous experiment,¹¹ and to the melting temperature of Bi under vacuum. For the RHEED streak intensity versus temperature

measurements, the electron gun is activated at a 1-kHz repetition rate with the frequency-quadrupled Nd:YAG laser. An example of an intensity versus temperature calibration is shown in Fig. 1. At least three calibrations were taken for each sample. The data are normalized to the streak intensity at the lowest temperature studied. The intensity of the diffraction pattern is consistent with Debye-Waller behavior up to the highest temperature studied, 523 K (i.e., the diffraction streak intensity attenuation is exponential with temperature indicating that no surface disordering occurs). The line fit of $\ln[I/I(T=300\text{ K})]$ versus T is forced through zero at the minimum temperature, and the best line fit is found by the method of least squares. The error bar is determined by the range of Debye temperatures calculated from all of the intensity calibration data. From the slope of the calibration a surface Debye temperature of 42 ± 9 K can be extracted, which is consistent with the previously reported value of $48\text{ K} \pm 20\%$ for Bi(0001) and Bi(01 $\bar{1}$ 2) using low-energy electron diffraction.¹⁴

We next discuss the time-resolved RHEED experiments. To determine the maximum superheating temperature, we observe the behavior of $I/I(T_{\text{bias}})$ versus peak laser intensity I_p for $T_{\text{bias}} = 523$ K at four different time delays. Figures 2(a)–2(d) show $\ln[I/I(T_{\text{bias}})]$ versus I_p for $t = t_0$, $t = t_0 + 0.5$ ns, $t = t_0 + 1.0$ ns, and $t = t_0 + 4.0$ ns, respectively, where t_0 is defined as the time of maximum modulation of $I/I(T_{\text{bias}})$ due to heating. The linear regions in Figs. 2(a)–2(d) show exponential decay consistent with Debye-Waller behavior. Deviation from this linear behavior is due to melting. By relating I_p to ΔT using Figs. 1 and 2(a), we confirm that the linear behavior of $\ln[I/I(T=523\text{ K})]$ versus I_p at $t = t_0$ is a continuation of the Debye-Waller effect observed below T_m within the experimental error. The line fits to the linear regions are forced through $\ln[I/I(T_{\text{bias}})] = 0$ when $I_p = 0$. In Fig. 2(a), the value of $\ln[I/I(T_{\text{bias}})]$ corresponding to the maximum I_p before deviation from linear

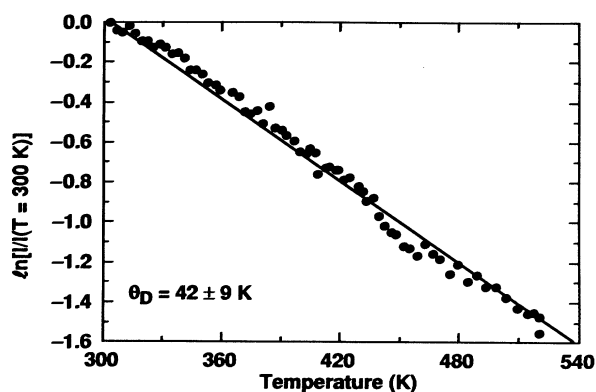


FIG. 1. A calibration is obtained to determine the temperature rise induced by the laser. We measure the intensity attenuation of the RHEED streaks as a function of surface temperature. The behavior of $\ln[I/I(T=300\text{ K})]$ vs T is consistent with the Debye-Waller effect throughout the temperature range studied. We obtain a surface Debye temperature of 42 ± 9 K for the Bi(0001) surface.

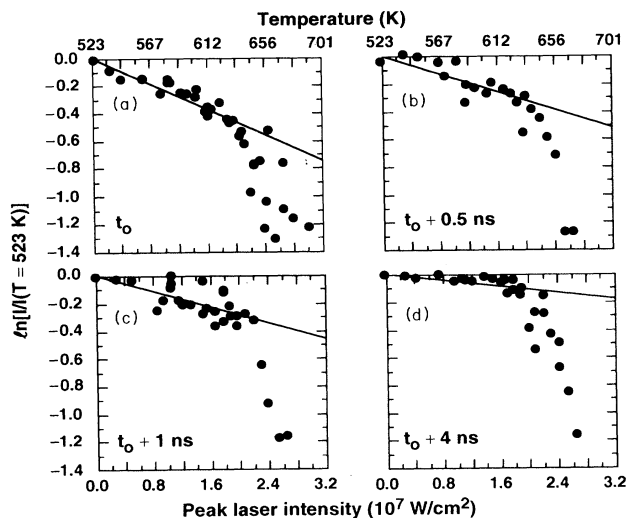


FIG. 2. The logarithm of the ratio of the heated streak intensity to the intensity at $T_{\text{bias}} = 523$ K is plotted vs peak laser intensity and temperature for (a) $t = t_0$, (b) $t = t_0 + 0.5$ ns, (c) $t = t_0 + 1.0$ ns, and (d) $t = t_0 + 4.0$ ns. Deviation from Debye-Waller behavior is seen, which corresponds to the onset of melting. Superheating of Bi(0001) occurs up until the break from the line fit that occurs at $2.0 \pm 0.2 \times 10^7$ W/cm² corresponding to a superheating temperature of 90 ± 25 K.

behavior is extracted and converted to a peak temperature rise ΔT , using the calibration in Fig. 1. The temperature axis is also given in Fig. 2. We find that for $T_{\text{bias}} = 523$ K, observation of melting occurs for $I_p = 2.0 \pm 0.2 \times 10^7$ W/cm². This corresponds to $\Delta T = 110 \pm 25$ K or, equivalently, a superheating temperature of 90 ± 25 K, not accounting for convolution effects. Included in this error bar is the range of temperatures obtained from the values of I_p corresponding to the point of deviation from Debye-Waller behavior in Fig. 2 (± 15 K), the error in converting diffraction intensity to temperature from the calibration of Fig. 1 (± 9 K), and the temperature uncertainty introduced by the spatial nonuniformity of the laser (± 15 K).

Ultrafast surface heating to peak temperatures below and above T_m is studied by temperature biasing the sample between room temperature and $T_m - 21$ K while monitoring the modulation of the streak intensity before, during, and after the arrival of the heating pulse. Figure 3 shows $I/I(T_{\text{bias}})$ versus delay time t . For $T_{\text{bias}} = 300$ K and $I_p = 2.0 \times 10^7$ W/cm² [Fig. 3(a)], the change in surface temperature ΔT at $t = t_0$ is approximately 115 K. The surface temperature remains below T_m . In Fig. 3(b), $T_{\text{bias}} = 429$ K and $I_p = 2.0 \times 10^7$ W/cm². The laser heating raises the surface temperature to $\sim T_m$. For $T_{\text{bias}} = 512$ K and $I_p = 2.0 \times 10^7$ W/cm² [Fig. 3(c)], the surface is heated to $\sim T_m + 90$ K, approximately the maximum observed superheating temperature. When $I/I(T_{\text{bias}})$ is converted to temperature using the calibration of Fig. 1, the temporal evolution of surface temperature is qualitatively consistent with a one-dimensional heat-diffusion model for Figs. 2(a)–2(c).^{15,16} For

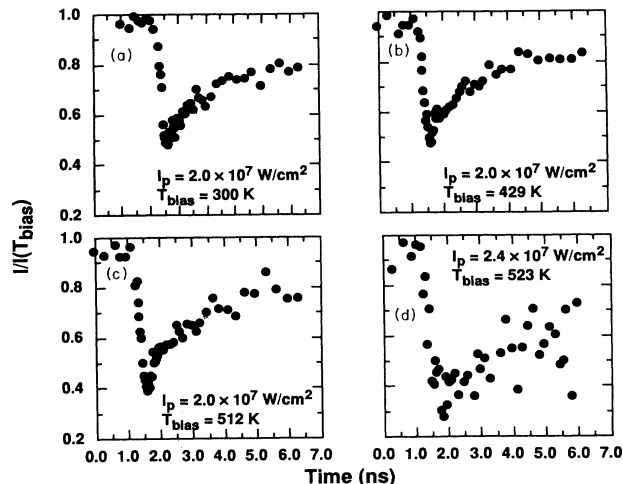


FIG. 3. The ratio of the heated streak intensity to the intensity at the bias temperature vs delay time is displayed for various bias temperatures. At temperatures below that of maximum superheating, the behavior is qualitatively consistent with a one-dimensional heat-diffusion model for laser heating both below and above T_m (a)–(c). Melting is evidenced in (d) as a deviation from this behavior.

$T_{\text{bias}} = 523$ K and $I_p = 2.4 \times 10^7$ W/cm² [Fig. 3(d)], the maximum superheating temperature is exceeded and melting occurs. This is indicated by a strong deviation from the behavior predicted by heat-diffusion model [i.e., difference in the behavior of Fig. 3(d) for large t when compared to Figs. 3(a)–3(c)] as well as visible laser damage to the surface. We monitor the sample visually to obtain a qualitative estimate of the threshold for laser damage and find that the earliest visual observations of damage coincide with the point at which $\ln[I/I(T_{\text{bias}})]$ versus I_p deviates from linear behavior.

After damage has occurred, the RHEED streaks are still visible but their intensities are diminished, indicating a reduction in the surface quality. We measure the reflectivity of the surface for $\lambda = 1.06$ μm at room temperature both before and after the occurrence of laser damage and find that the reflectivity has decreased from 0.67 to 0.49. SEM images of the laser-damaged surface indicate that the surface has melted. The SEM images show the formation of a periodic structure with periodicity about equal to the wavelength of the laser. This periodic structure forms in a hexagonal arrangement of melt puddles, which in some regions coalesce into parallel rows. The spacing between puddles and rows is approximately equal to the wavelength of the heating laser.

Previous pulsed-laser melting experiments on the (0001), ($\bar{1}010$), and ($2\bar{1}\bar{1}0$) surfaces of Bi with a ruby laser with a 30-ns pulse width have shown defect formation on the ($\bar{1}010$) and ($2\bar{1}\bar{1}0$) surfaces resulting from mechanical stress induced by slip planes parallel to the (0001) surface. In these experiments, the Bi(0001) surface regrew epitaxially from the liquid with no laser-induced periodic surface structure observed.¹⁷ The different behavior observed in our experiments may be related to the two-orders-of-magnitude difference in pulse width.

In the previous superheating experiments on Pb(111),¹⁰ surface damage was only induced by the laser for an I_p much larger than that which corresponded to maximum superheating. However, this damage could be removed by pulsed-laser melting above the superheating threshold. For Pb(111) the threshold for pulsed-laser melting is lower than the threshold for pulse-laser damage although for Bi(0001) these two thresholds appear to be comparable.

In conclusion, using time-resolved RHEED we have observed superheating of Bi(0001) by 90 ± 25 K. For laser heating corresponding to a larger ΔT , melting is observed as a deviation from Debye-Waller behavior. For these

larger heatings, irreversible laser damage resulting in a hexagonal periodic surface structure is also observed. Bi and Pb experience very different properties associated with bulk melting, such as volume change and change in electrical and thermal conductivities.¹⁸ Therefore, our observation of superheating of Bi(0001), coupled with the previously observed superheating of Pb(111),¹⁰ suggests the generality of the superheating phenomenon.

This work was supported by the U.S. Department of Energy under Contract No. DE-FG02-88ER45376. We gratefully acknowledge J. Chu at the University of Illinois for the SEM work.

¹G. D. T. Spiller, *Philos. Mag. A* **46**, 535 (1982).

²J. J. Métois and J. C. Heyraud, *J. Phys. (Paris)* **50**, 3175 (1989).

³S. J. Peppiatt, *Proc. R. Soc. London Ser. A* **345**, 401 (1975).

⁴M. Blackman, S. J. Peppiatt, and J. R. Sambles, *Nature (Phys. Sci.)* **239**, 61 (1972).

⁵J. Däges, H. Gleiter, and J. H. Perepezko, in *Phase Transitions in Condensed Systems—Experiments and Theory*, edited by G. S. Cargill, F. Spaepen, and K.-N. Tu, MRS Symposia Proceedings No. 57 (Materials Research Society, Pittsburgh, 1987), p. 67.

⁶S. E. Kaykin and N. P. Bene, *C. R. Acad. Sci. USSR* **23**, 31 (1939).

⁷A. P. Baikov and A. G. Shestak, *Pis'ma Zh. Tekh. Fiz.* **5**, 1355 (1979) [*Sov. Tech. Phys. Lett.* **5**, 569 (1979)].

⁸C. J. Rossouw and S. E. Donnelly, *Phys. Rev. Lett.* **55**, 2960 (1985).

⁹L. Gråbaek, J. Bohr, E. Johnson, A. Johansen, L. Sarholt-Kristensen, and H. H. Andersen, *Phys. Rev. Lett.* **64**, 934 (1990).

¹⁰J. W. Herman and H. E. Elsayed-Ali, *Phys. Rev. Lett.* **69**, 1228 (1992).

¹¹J. W. Herman and H. E. Elsayed-Ali, *Phys. Rev. Lett.* **68**, 2952 (1992).

¹²J. D. Mackenzie and R. L. Cormia, *J. Chem. Phys.* **39**, 250

(1963).

¹³H. E. Elsayed-Ali and J. W. Herman, *Rev. Sci. Instrum.* **61**, 1636 (1990).

¹⁴R. M. Goodman and G. A. Somorjai, *J. Chem. Phys.* **52**, 6325 (1970).

¹⁵For Bi(0001) at $T = 300$ K we use $\alpha = 5.93 \times 10^7 \text{ m}^{-1}$, $K = 8.25 \text{ W/mK}$, and $C = 1.16 \times 10^6 \text{ J/m}^3 \text{ K}$ from J. N. Hodgson, *Proc. Phys. Soc. (London) B* **67**, 269 (1954); and *Thermophysical Properties of Matter*, edited by Y. S. Touloukian (Plenum, New York, 1970), Vols. 1 and 2. $R = 0.67$ is experimentally determined.

¹⁶J. H. Bechtel, *J. Appl. Phys.* **46**, 1585 (1975).

¹⁷A. L. Helms, Jr., C. W. Draper, D. C. Jacobson, J. M. Poate, and S. L. Bernasek, *J. Mater. Res.* **3** (1988); A. L. Helms, Jr., C.-C. Cho, S. L. Bernasek, C. W. Draper, D. C. Jacobson, and J. M. Poate, in *Laser Surface Treatment of Metals*, edited by C. W. Draper and P. Mazzoldi (Nijhoff, Dordrecht, 1986); A. L. Helms, Jr., C. W. Draper, D. C. Jacobson, J. M. Poate, and S. L. Bernasek, in *Energy Beam-Solid Interactions and Transient Thermal Processing*, edited by D. K. Biegelsen, G. A. Rozgonyi, and C. V. Shank, MRS Symposia Proceedings No. 35 (Materials Research Society, Pittsburgh, 1985), p. 439.

¹⁸B. R. T. Frost, *Prog. Met. Phys.* **5**, 96 (1954).